**Nuclei Shapes across Different Magic Numbers in the Ytterbium (Z = 70) and Lead (Z = 82) Isotopes using MATLAB Code.**

**Eriba-Idoko F.[1], Daniel, T.[1], Gbaorun, F.[1] and Hemba, E. C.[2]**
1. Department of Physics, Benue State University, P.M. B. 102119, Makurdi.
2. Department of Physics, Federal College of Pankshin, Plateau State.
*Corresponding author's email: tdaniel@bsum.edu.ng, Tel: 08167598988

**Abstract**

The yrast state of the$Ytterbium, Yb$ isotopes for the neutron range of $82 \leq N \leq 108$and $Lead$, $Pb$isotopes for the neutron range of $98 \leq N \leq 132$for the even-even nuclei have been studied using the energies of the first excited state in these nuclei. The nuclear deformation parameters, $\beta_2$ and the reduced quadruple transition probability $B(E2) \uparrow$ with other intrinsic parameters associated with the nuclei shape were obtained using a MATLAB code.The results revealed that the $Pb$ nucleus with Z = 82 - which is one of the magic numbers have a more 'spherically' nuclei shape at the ground state with small degree of deformation as compared to the nuclei shapes in the $Yb$isotopes. Our studysupports the global predictions of the prolate deformation in$Yb$ isotopes around the neutron range of$90 \leq N \leq 112$.

**Keywords**: Excited energies, Magic numbers, Deformation parameter, Semi-major and Semi-minor axis

## Introduction

Increase in excitation energies and or the angular momenta can bring about a change in the nuclear shape of a nucleus (Casten, 2000; Casten *et. al*, 2009). Such changes are caused by rearranging the orbital configuration of the nucleus or by the dynamic response of the nuclear system to rotation. Nuclear shapes can also be caused about as a result of an increase or decrease in proton or neutron number (Flavigny *et. al*, 2017; Daniel *et. al*, 2019). The deformation can be described by a multipole extension, such as the quadrupole and octupole deformation, with the quadrupole deformation being the most important deformation from spherical shape to oblate or prolate shape (Garcia-Ramos et. al, 2013; Garcia-Ramos *et. al*, 2014). Such quadrupole shapes have axial symmetry. The most commonly experienced shapes called the elongated (prolate) and prostrated (oblate) shapes are shown in Figure 1.

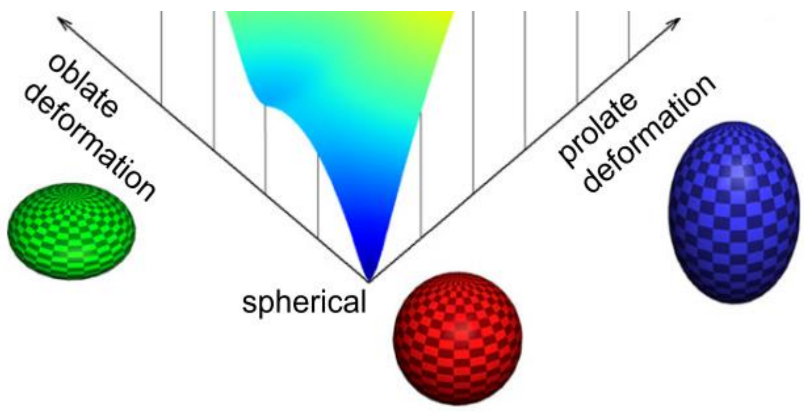


**Figure 1:** Schematics images of nuclear shapes (Otsuka, et al, 2016; Daniel, 2017)

In this work, we present nuclei shapes and shape transitions across different magical "extremes" of proton number $Z = 82$ and neutron number$N = 82$ and 126 for even-even nuclei of $Ytterbium$ isotopes($^{152-178}_{70}\boldsymbol{Yb}_{82-108}$)and $Lead$ isotopes ($^{180-214}_{82}\boldsymbol{Pb}_{98-132}$) by determining thenuclear deformation parameters, $\beta_2$, the reduced quadrupole transition probability $B(E2)\uparrow$, semi-major axis, $a$, and semi-minor axis, $b$, with other intrinsic parameters associated with nuclei isotopes from the energies of the $2^+$excited states by the instrumentality of the MATLAB code. These shapes were further revealed by the plot of two dimensional axially symmetric quadrupoleprolate shapes using the semi-minor and the semi-major axis as calculated for these nuclei.

## Nuclear Reaction Mechanisms

The large percentage of the knowledge of the properties of nucleus is derived from nuclear reactions (Wong, 2004). The nuclear excited energies of the yrast $2^+$state as retrieved from National Nuclear Data Center (NuDat2.6, 2018; Segre Chart, 2019) emanated from nuclear reaction processes such as the coulomb excitation and fusion evaporation reactions.

### Coulomb Excitation Reaction

Coulomb excitation reaction is purely an electromagnetic interaction process due to the presence of coulomb field that exist between the two colliding nuclei. Here, stable target are bombarded with heavy ions at energies that are less than the coulomb barrier energy such that, the coulomb repulsion prevents the particles from touching each other, thus ensuring a pure coulomb excitation process (Clement, 2007).The coulomb barrier of a particular target nuclei can be estimated from the equation(Regan, 2003);

$$V_c = \frac{Z_1 Z_2 e^2}{4\pi\varepsilon_0 R} = 1.442\frac{Z_1 Z_2}{R} \qquad (1)$$

Where $R$ (in units of *fm*) is known to be the separation distance defined as

$$R = 1.36\left(A_1^{1/3} + A_2^{1/3}\right) + 0.5 \qquad (2)$$

and $Z_1$ and $Z_2$ are the proton numbers, $A_1$ and $A_2$ are the mass numbers for the beam and the target nuclei, respectively. $\varepsilon_0 = 8.854 \times 10^{-12} fm^{-1}$ is the permittivity of free space and $e$ is the electronic charge in units of Coulombs (C).

**Fusion Evaporation Reaction**

A compound nucleus can be formed by bombarding a beam of particles on a target nucleus. If the energy of the projectile particle is enough to overcome the Coulomb barrier of the target nucleus given by Eqn. (1), then projectile nucleus (i.e. beam) fuses with the target nucleus momentarily (Hodgson *et. al,* 1997). This resulting compound nucleus subsequently decays after sharing energy among the constituent nucleons, to a lower energy state. The reaction process is represented by;

$$p + T \rightarrow C^* \rightarrow R + x \qquad (3)$$

Where $p$ is the projectile nucleus (the beam), $T$ is the target nucleus, $R$ is the daughter nucleus, $x$ is the emitted or evaporated particle and $C^*$ is the compound nucleus formed in the reaction. The decay process of the compound nuclei proceeds by emission of particles such as neutrons, protons, deuterons and $\alpha$-particles. When the excitation energy of the residual is below the particles binding energy, these residual nuclei de-excite by emission of cascade of γ-rays until the residual nuclei reach their ground states (Krane, 1988).The γ-rays are detected using nuclear detectors. The energies of the emitted γ-rays which also corresponds to the excited energies are then measure in the order of $keV$.

Figure 2 is the low-lyingenergy level spectrum for even-even $Yb$ isotopes (Figure 2a) and $Pb$ Isotopes (Figure 2b), showing the nuclear decay process from the $E(4^+)$ excited state through the yrast $E(2^+)$ excited state to the ground state. A succession of two stages of decay process (i.e. the nucleus decay from $E(4^+)$ excited state to the $E(2^+)$ state and then, to the ground state) may be preferable to a single decay process from $E(4^+)$ state to the ground state depending on the intensities of the emitted γ-rays.

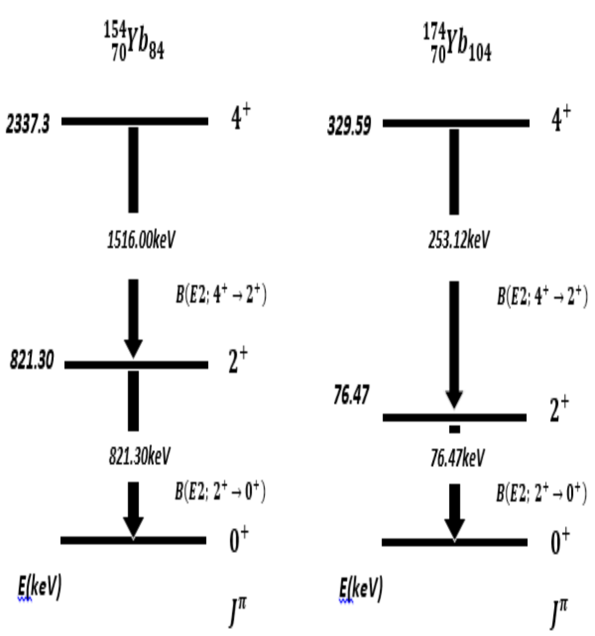


Figure 2a: Nuclear decay process for Yb isotopes showing excited energies. *E (keV)* is retrieved from (NuDat2.6, 2018)

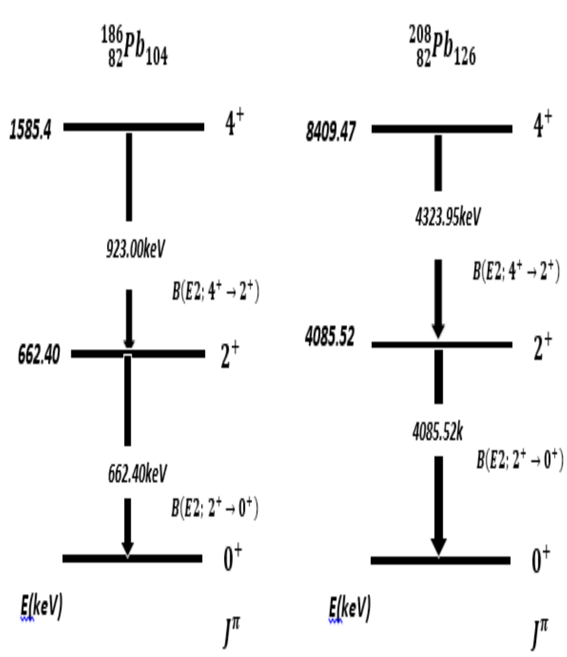


Figure 2b: Nuclear decay process for Pb isotopes showing excited energies. *E (keV)* is retrieved from (NuDat2.6, 2018)

**Method of Data Extraction, Analysis and Calculation of Nuclear Parameters**

The data set for the gamma energies of the $2^+$ excited state were extracted from Brookhaven Nuclear Laboratory BNL (NuDat2.6, 2018) for the thirty-two (32) even-even nuclei of *Ytterbium* isotopes $({}^{152-178}_{70}\boldsymbol{Yb}_{82-108})$and *Lead* isotopes $({}^{180-214}_{82}\boldsymbol{Pb}_{98-132})$ under study.

Nuclear signatures for shape transitions can be observed from the values of the deformation parameters,$\beta_2$, which is connected to a sudden change in the mean square charge radius and an associated change in the intrinsic quadruple moments, $Q_0$. The axially symmetric deformed nuclear shape is explained by the deformation parameters. The intrinsic quadruple moment also plays a definitive role in determining the reduced quadruple transition probability, $B(E2)\uparrow$ from the energies of the low-lying nuclear excited states. The reduced element transition probability, $B(E2)\uparrow$ from the spin/parity $0^+$ ground state to the first excited spin/parity $2^+$ state is related to the intrinsic quadruple moments $Q_0$ by (Audi *et al*, 2003;Pritychenko, et al., 2016 ):

$$B(E2; 0^+_{gs} \to 2^+_1) = \frac{5}{16\pi} e^2 Q_0^2 \qquad (4)$$

Where $Q_0$is in unit of barn (b). If $Q_0$ is considered to be calculated for a homogenously charged ellipsoid with charge *Ze* and with the semi-major *'a'* and semi-minor *'b'* axes pointing along the *z*-axis, $Q_0$ is given by (Krane, 1988; Henley et al, 2007);

$$Q_0 = \frac{2}{5} Z(a^2 - b^2) \qquad (5)$$

For a negligible deviation from sphericity, $Q_0$ can be presented in terms of the distortion parameter $\delta$ as

$$Q_0 = \frac{4}{5} ZR^2\delta \qquad (6)$$

where$R = R_o A^{\frac{1}{3}}$ is the radius of sphere. The nuclear quadruple distortion parameter values $\delta$ are calculated from the equation

$$\delta = \frac{0.75 Q_0}{Z(< r^2 >)} \qquad (7)$$

where the parameter,$< r^2 >$ is known as the mean square charge radius and is deduced directly from (Krane, 1988).

$$< r^2 > = \frac{3}{5} R^2 = \frac{3}{5} R_0^2 A^{2/3} \qquad (8)$$

Equations (7) and (8) have been used to obtain the semi major axis *'a'* and semi minor axis *'b'* for the Ytterbium isotopes from the relation.

$$a = \sqrt{< r^2 > \left(1.66 - \frac{2\delta}{0.9}\right)} \qquad (9)$$

and

$$b = \sqrt{5 < r^2 > -2a^2} \qquad (10)$$

The $B(E2)\uparrow$ values are requisite experimental quantities that do not depend on nuclear models but depend so perfectly on the quadrupole deformation parameter by the relation (Raman, 2002; Ertugral, et. al., 2015; Daniel, 2017)

$$\beta_2 = \left(\frac{4\pi}{3zR_0^2}\right) [\, B(E2) \uparrow / e^2]^{\frac{1}{2}} \qquad (11)$$

where the nuclear radius,

$$R_0^2 = 1.2 \times A^{1/3} fm)^2 = 0.0144 A^{2/3} b \qquad (12)$$

The excited energy of the $2^+$ state *E(2⁺) (keV)* is all that is required to obtain the corresponding *B(E2)↑ (e²b²)* values for the Ytterbium and Lead isotopes. They are related by;

$$B(E2) \uparrow = 2.6 E_\gamma^{-1} Z^2 A^{-\frac{2}{3}} \qquad (13)$$

where$E_\gamma$ in equation (13) corresponds to the excited energy of the $2^+$ state, $E(2^+)$ *(keV)*.

The deformation parameters ($\beta_2$) derived from *B(E2)↑* for even-even nuclei for the *Yb* isotopes and *Pb* isotopes were calculated using equation (11). The *B(E2)↑*from the ground state to the first excited $2^+$ state were calculated using equation (13). The average nuclear radius $R_o^2$ and the distortion parameter $\delta$, were obtained using Eqns. (12) and (7) respectively, while the various parameters of the intrinsic quadrupole moment, $Q_0$ and the mean square charge radius, $<r^2>$ were obtained from equations (4) and (8), respectively. The semi-major axis, *a* and the semi-minor axis, *b* were also obtained using equation (9) and (10), respectively. Also, the difference between the major and the minor axes,

$\Delta R$ between $a$ and$b$ was calculated. A MATLAB code was developed to analyze and evaluate the above nuclear parameters. These parameterswere analysed in such a way that, for a particular nucleus in the selected range(32 even-even nuclei isotopes all together), its excited energy value$E(2^+)$ isused to obtain its associated intrinsic nuclear parameters (such as $\beta_2$, $B(E2)\uparrow$, $Q_0$, $\delta$ etc.). The same procedure was repeated for the remaining thirty-one (31) nuclei.

## Results and Discussion

### Results

The evaluated intrinsic nuclear parameters are presented in Table 1 and the resulting two dimensional axially symmetric quadrupole deformed nuclei shapes for ${}^{152-178}_{70}Yb$ and ${}^{180-214}_{82}Pb$isotopes are shown in Figures (3 – 12).

**Table 1:** The values of the $B(E2)\uparrow(e^2b^2)$,$Q_0(b)$ and other intrinsic parameters of the selected $_{70}Yb$ and $_{82}$Pb nuclei isotopes obtained using MATLAB.

| *A* | *N* | *E(2⁺)(KeV)* | *B(E2)↑ (e²b²)* | *Q₀(b)* | *β₂* | *δ* | *R₀²(fm)* | *⟨r²⟩^1/2 (fm)* | *a (fm)* | *b (fm)* | *ΔR(fm)* |
|---|---|---|---|---|---|---|---|---|---|---|---|
| | | | | | **$_{70}$Yb** | | | | | | |
| 152 | 82 | 1531.40 | 0.292 | 1.714 | 0.079 | 0.075 | 0.410 | 4.956 | 3.236 | 3.755 | 0.519 |
| 154 | 84 | 821.30 | 0.540 | 2.330 | 0.106 | 0.101 | 0.414 | 5.043 | 3.201 | 3.895 | 0.694 |
| 156 | 86 | 536.40 | 0.820 | 2.870 | 0.130 | 0.123 | 0.417 | 5.131 | 3.172 | 4.019 | 0.846 |
| 158 | 88 | 358.20 | 1.217 | 3.498 | 0.157 | 0.148 | 0.421 | 5.218 | 3.133 | 4.155 | 1.022 |
| 160 | 90 | 243.10 | 1.778 | 4.228 | 0.188 | 0.178 | 0.424 | 5.307 | 3.081 | 4.306 | 1.225 |
| 162 | 92 | 166.85 | 2.569 | 5.082 | 0.224 | 0.212 | 0.428 | 5.395 | 3.012 | 4.473 | 1.462 |
| 164 | 94 | 123.36 | 3.447 | 5.887 | 0.258 | 0.244 | 0.431 | 5.484 | 2.945 | 4.629 | 1.684 |
| 166 | 96 | 102.37 | 4.120 | 6.436 | 0.279 | 0.264 | 0.435 | 5.574 | 2.908 | 4.743 | 1.835 |
| 168 | 98 | 87.73 | 4.770 | 6.925 | 0.298 | 0.282 | 0.438 | 5.663 | 2.877 | 4.847 | 1.970 |
| 170 | 100 | 84.25 | 4.928 | 7.038 | 0.301 | 0.284 | 0.442 | 5.753 | 2.892 | 4.894 | 2.002 |
| 172 | 102 | 78.74 | 5.231 | 7.252 | 0.307 | 0.291 | 0.445 | 5.844 | 2.895 | 4.956 | 2.062 |
| 174 | 104 | 76.47 | 5.345 | 7.331 | 0.308 | 0.292 | 0.449 | 5.935 | 2.914 | 4.998 | 2.084 |
| 176 | 106 | 82.13 | 4.939 | 7.047 | 0.294 | 0.278 | 0.452 | 6.026 | 2.979 | 4.985 | 2.006 |
| 178 | 108 | 84.00 | 4.793 | 6.941 | 0.288 | 0.272 | 0.456 | 6.117 | 3.022 | 4.999 | 1.978 |
| | | | | | **$_{82}$Pb** | | | | | | |
| 180 | 98 | 1168.00 | 0.470 | 2.173 | 0.076 | 0.072 | 0.459 | 8.781 | 3.629 | 4.191 | 0.562 |
| 182 | 100 | 888.30 | 0.613 | 2.482 | 0.086 | 0.082 | 0.462 | 8.911 | 3.629 | 4.267 | 0.638 |
| 184 | 102 | 701.50 | 0.770 | 2.783 | 0.096 | 0.091 | 0.466 | 9.042 | 3.630 | 4.342 | 0.711 |
| 186 | 104 | 662.40 | 0.810 | 2.854 | 0.098 | 0.093 | 0.469 | 9.173 | 3.652 | 4.381 | 0.729 |
| 188 | 106 | 723.60 | 0.736 | 2.720 | 0.093 | 0.088 | 0.473 | 9.305 | 3.692 | 4.389 | 0.697 |
| 190 | 108 | 773.90 | 0.684 | 2.621 | 0.089 | 0.084 | 0.476 | 9.437 | 3.729 | 4.402 | 0.673 |
| 192 | 110 | 853.64 | 0.615 | 2.487 | 0.084 | 0.079 | 0.479 | 9.570 | 3.769 | 4.409 | 0.641 |
| 194 | 112 | 965.08 | 0.541 | 2.331 | 0.078 | 0.074 | 0.483 | 9.703 | 3.810 | 4.413 | 0.603 |
| 196 | 114 | 1049.20 | 0.494 | 2.228 | 0.074 | 0.070 | 0.486 | 9.837 | 3.847 | 4.425 | 0.578 |
| 198 | 116 | 1063.50 | 0.484 | 2.206 | 0.073 | 0.069 | 0.489 | 9.971 | 3.877 | 4.449 | 0.573 |
| 200 | 118 | 1026.61 | 0.498 | 2.237 | 0.073 | 0.069 | 0.492 | 10.105 | 3.901 | 4.482 | 0.581 |
| 202 | 120 | 960.67 | 0.529 | 2.305 | 0.075 | 0.071 | 0.496 | 10.240 | 3.922 | 4.520 | 0.597 |
| 204 | 122 | 899.17 | 0.561 | 2.375 | 0.077 | 0.073 | 0.499 | 10.376 | 3.943 | 4.558 | 0.615 |
| 206 | 124 | 803.05 | 0.624 | 2.505 | 0.080 | 0.076 | 0.502 | 10.512 | 3.959 | 4.606 | 0.647 |
| 208 | 126 | 4085.52 | 0.122 | 1.107 | 0.035 | 0.033 | 0.506 | 10.648 | 4.109 | 4.412 | 0.303 |
| 210 | 128 | 799.70 | 0.619 | 2.494 | 0.079 | 0.075 | 0.509 | 10.785 | 4.014 | 4.658 | 0.644 |
| 212 | 130 | 804.90 | 0.611 | 2.478 | 0.078 | 0.074 | 0.512 | 10.922 | 4.042 | 4.683 | 0.641 |
| 214 | 132 | 835.00 | 0.585 | 2.425 | 0.076 | 0.072 | 0.515 | 11.059 | 4.074 | 4.702 | 0.628 |

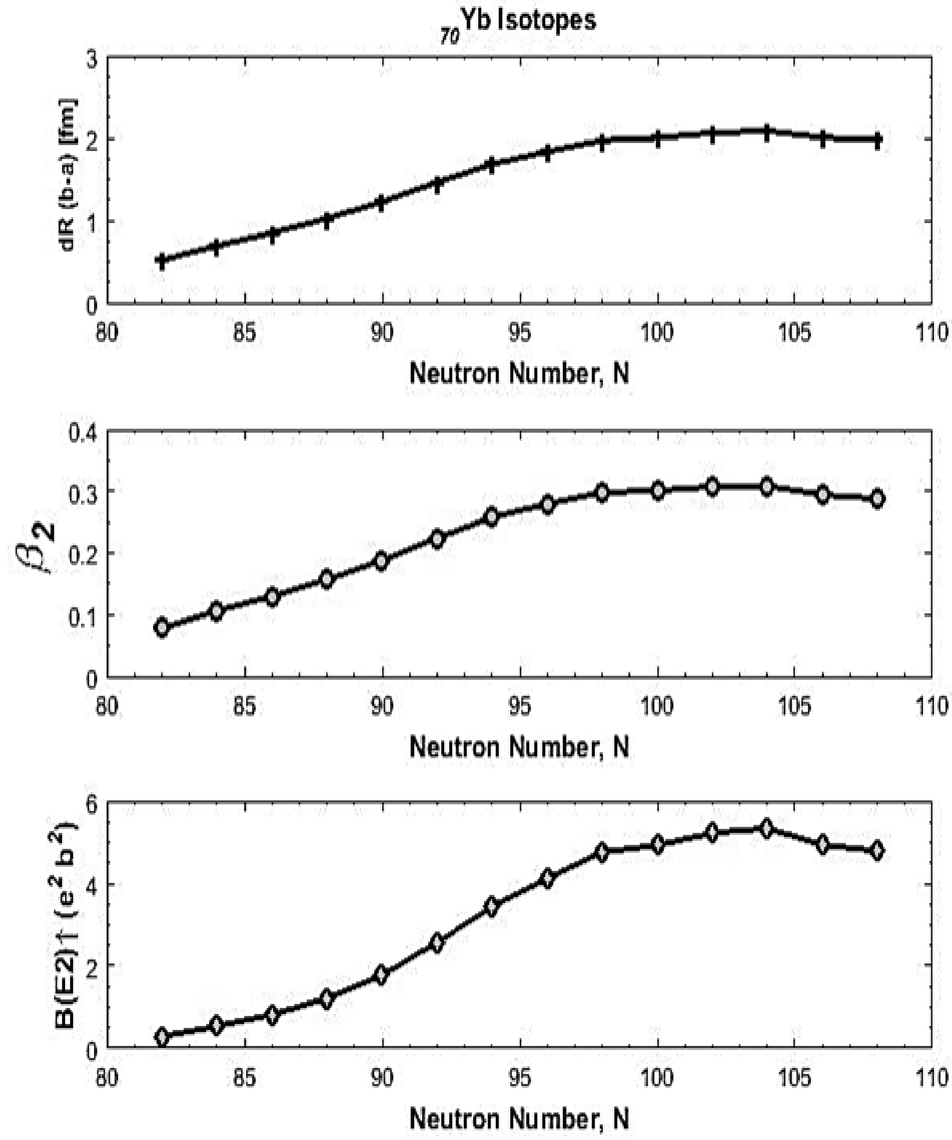


**Figure 3:** Deformation parameter $\beta_2$ and the reduced quadrupole transition probability *B(E2)* plotted against neutron number N for the $_{70}Yb$ nuclei $82 \leq N \leq 108$

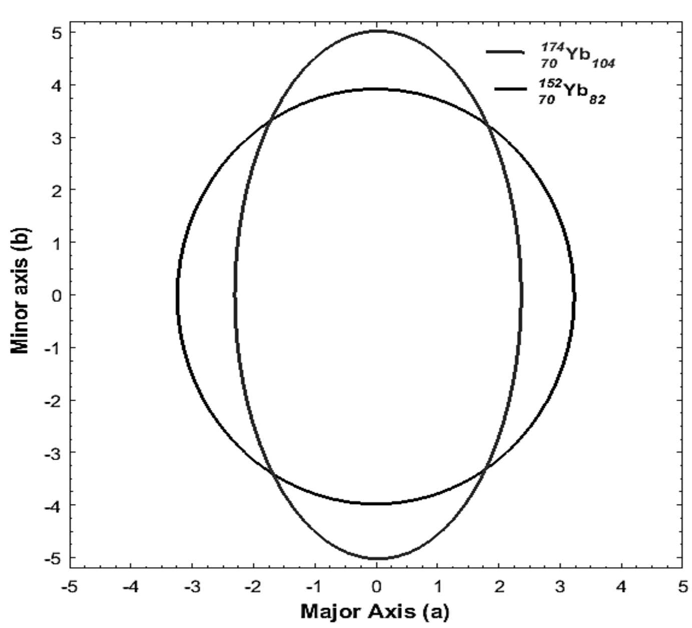


**Figure 4:** 2D plot of axially symmetric quadruple deformation about magical 'extremes' of $_{70}Yb$, for N = 82 (magic number) and 104.

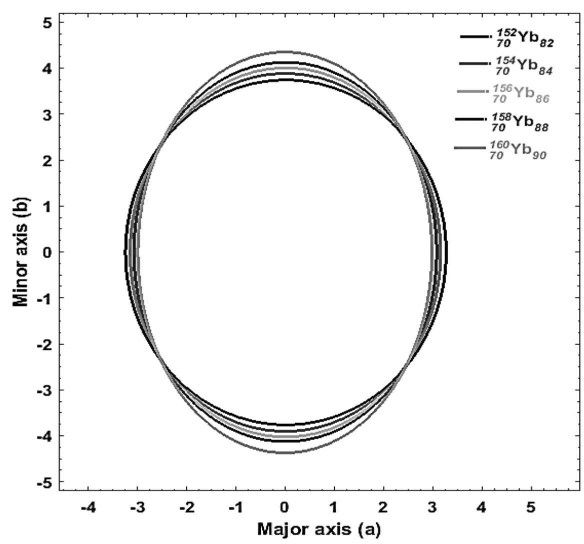


**Figure 5**: 2D plot of axially symmetric quadruple deformation of $_{70}Yb$ nuclei for $82 \leq N \leq 90$

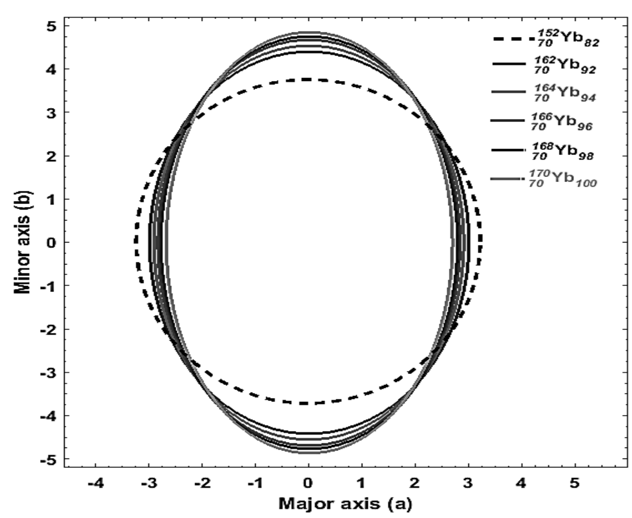


**Figure 6:** 2D plot of axially symmetric quadruple deformation of $_{70}Yb$ nuclei for $92 \leq N \leq 100$

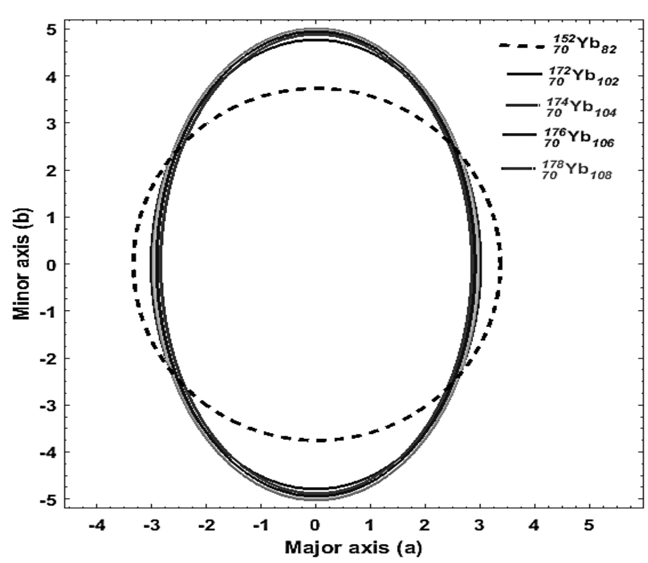


**Figure 7:** 2D plot of axially symmetric quadruple deformation of $_{70}Yb$ nuclei for $102 \leq N \leq 108$.The dotted 2D plot is that of the singly magic nucleus of Yb.

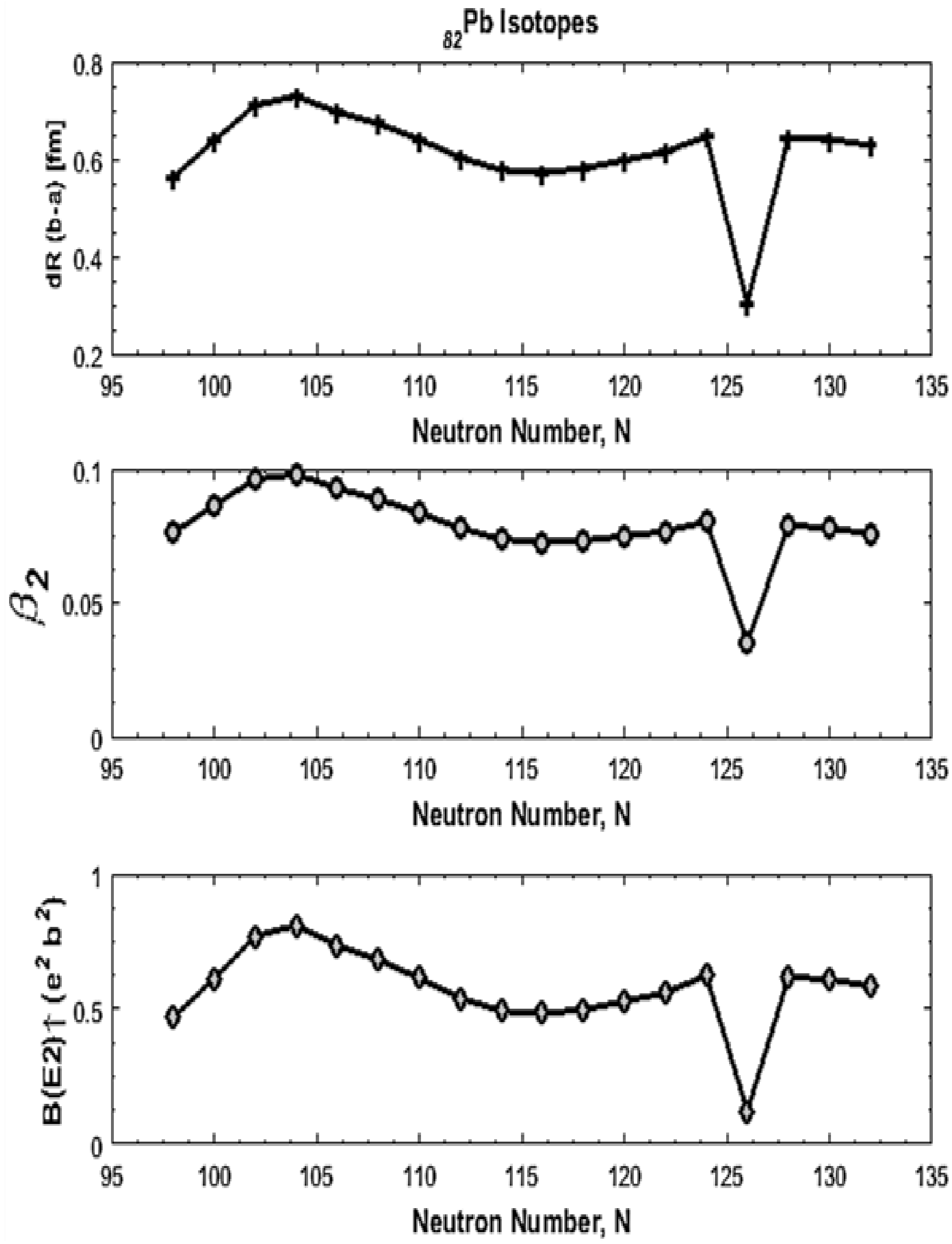


**Figure 8:** Deformation parameter $\beta_2$ and the reduced quadrupole transition probability *B(E2)* plotted against neutron number N for the $_{82}Pb$ nuclei for $98 \leq N \leq 214_{82}$ Pb *nuclei*

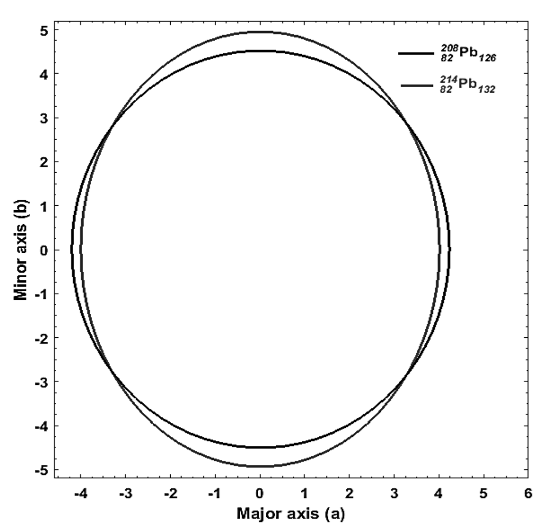


**Figure 9:** 2D plot of axially symmetric quadruple deformation of $_{82}Pb$ nuclei about $N = 126$ and $N = 132$

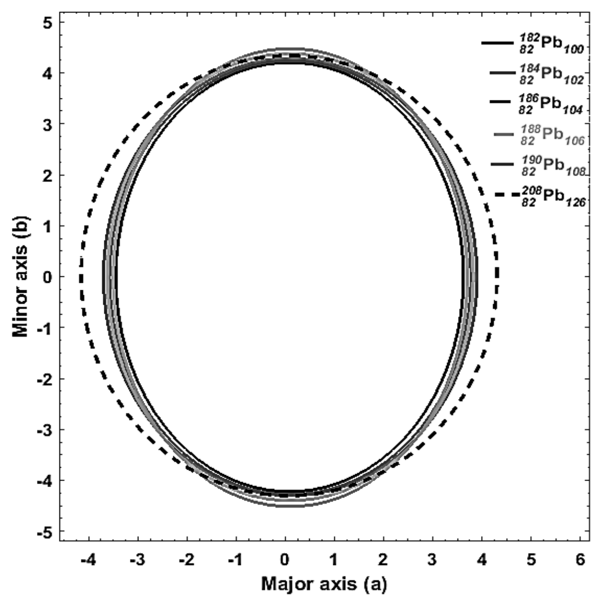


**Figure 10:** 2D plot of axially symmetric quadruple deformation of $_{82}Pb$ nuclei for $100 \leq N \leq 108$

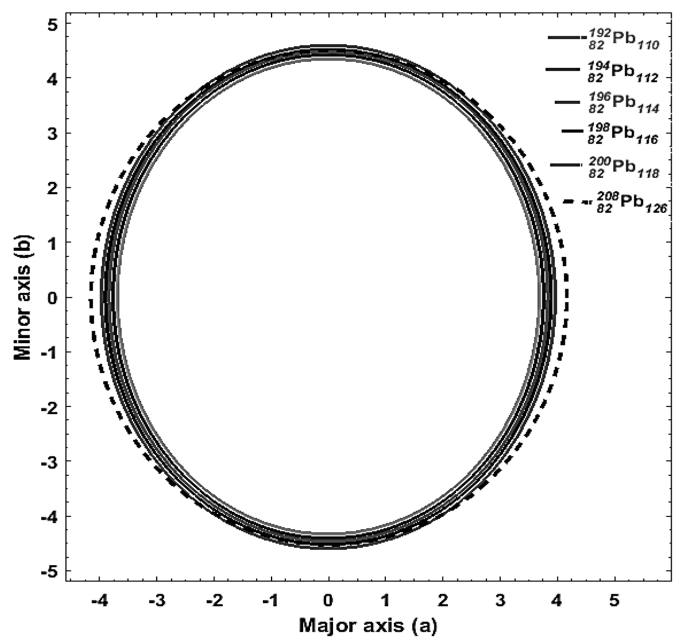


**Figure 11:** 2D plot of axially symmetric quadruple deformation of $_{82}Pb$ nuclei for $110 \leq N \leq 118$

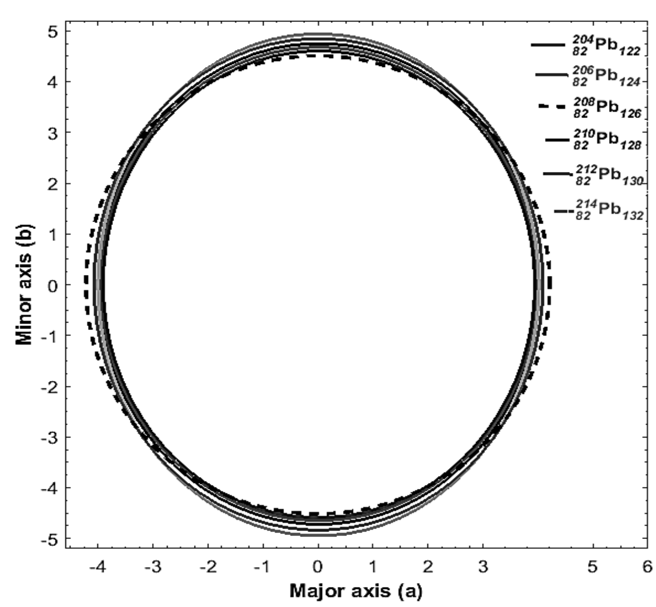


**Figure 12:** 2D plot of axially symmetric quadruple deformation of $_{82}Pb$ nuclei for $122 \leq N \leq 132$

## Discussion

The discussion of the changing nuclei shape behavior or simply the nuclei shape evolution is based on either the addition or removal of the neutron number(s) from the isotope.

As presented in Table 1, the values of the$Q_0$, $B(E2)\uparrow$,$\beta_2$, and $\Delta R$for the isotopes of Ytterbium have been obtain edusing MATLAB code. It has been observed that the higher the energy of the $2^+$ state in the nucleus, the smaller the $\Delta R$values from $N = 82$to $N = 104$. As this trend changes from $N = 106$ and beyond, the values of $\Delta R$ experience an upward increase, thereby confirming the fact that the neutron number is now pointing towards the next magic number of 126. While this happens, nuclei isotopic shape also changes from almost being spherical to a more prolate –oblate shape detailing much information about the 'deformation' in the nucleus of the atom.

In the isotopes of Ytterbium presented here (in Table 1), the isotope with $N = 82$ (a magic neutron number) has the smallest of $\Delta R$ as 0.519*fm*, and as the neutron number move away from the magic 82, this values increases upward. This confirms nuclei shape evolution. (see Figures 4 to 7 for details).

The same scenarios is presented for the Lead isotopes in Table 1. In this presentation however, the smallest value of$\Delta R$ is 0.303 *fm*at $N = 126$ (and even in comparison with the 0.519*fm* value obtained in the $Yb$ isotope at $N = 82$ – which is only magic in that neutron number). The doubly magic number in the lead isotope of $^{208}_{82}Pb_{126}$with $Z = 82,$ and $N = 126$has contributed to the spherical nature of its shape. Thus, the lower of $\Delta R$.And because the nucleons are all magic, it requires a higher amount of energy to knock out a neutron or to excite the nucleus to higher energy levels. For instance, at $N = 126$ in the Pb, the energy required to excite the nuclei to the yrast $2^+$ state is 4085.52 *keV* higher than any other isotope in Pb (see Figure 8 for details). In Figure 8, the presence of these magic numbers in $Pb$ have made the *B(E2)* and the$\beta_2$values minimum as being plotted against neutron number. Figures 9 – 12 have presented the various prolate shapes of the nuclei with addition of more neutrons which confirms the experimental results presented in reference(NuDat2.6, 2018; Daniel et al., 2017; Segre Chart, 2019), where the nuclei maintained a prolately deformed shape within the range $90 \leq N \leq 112$ with corresponding Protons, Z in range of$50 \leq Z \leq 80$.

## Conclusion

The presence of the doubly magic number $Z = 82$ and $N = 126$ in the $Lead$ nuclei is the determining factors for the shape where most of the isotopes are found to be more spherical compared to the $Ytterbium$ isotopes where $Z = 70$ which is 12 protons away from the $Z = 82$ as in the case of $Lead$.Thus, $Lead$ nuclei is more stable with almost all isotopes of nearly closed shell and undergo very small deformation from sphericity with changing neutron numbers. This property must have accounted for why$Lead$is a good material for shielding gamma rays.

## Acknowledgement

TD would like to acknowledge Prof. Patrick H. Regan for introducing him to the study of nuclear systematics and coincidence technique measurement. TD would also wish to thank the staff of the IFIN-HH Nuclear Physics Laboratory, Bucharest, Romania for allowing him access to the Lab for his Ph.D. work and assistance during data analysis.FEI wish to thank Dr. Terver Daniel his project supervisor who inculcates him with necessary research skills, Frederick Gbaorun for painstakingly reviewing this article and also Mr. AnejoItodo for introducing him to MATLAB programming.

## References

Audi, G., Bersillonb, O., Blachotb, J. and Wapstrac, A.H. (2003).The NUBASE evaluation of nuclear and decay properties, *Journal of Nuclear Physics*, A 729, 3–128.

Casten, R. F. and Cakirli, R. B. (2009). Evolution of structure in nuclei: meditation by sub-shell modifications and relation to binding energies, *ActaPhysicaPolonia*, B 40, 493-502

Casten, R.F. (2000). Nuclear Structure from a Simple Perspective, Oxford Science Publications, 2nd Edition.

Clement, E. (2007). Exotic shapes in exotic nuclei: Shape coexistence in unstable nuclei studied by Coulomb excitation. Seminar presentation at CERN-PH/IS, France. https://indico.cern.ch/event/432094/attachments/937081/1327656/EP-Seminaire.pdf

Daniel, T (2017). Nuclear Structure Studies of Low-lying States in 194Os Using Fast-Timing Coincidence Gamma-ray Spectroscopy PhD Thesis. Submitted to the University of Surrey, Guildford, UK.

Daniel, T., Eriba-Idoko, F. and Gbaorun, F. (2019). Review of the Nuclear Systematics for Nuclei A ≈ 140 - 214, *Journal of Nigerian Association of mathematical physics*, *JNAMP* Vol. 49: 251 – 256. http://e.nampjournals.org/product-info.php?pid3771.html

Daniel, T., Kisyov, S., Regan, P. H., Marginean, N., Podolýak, Z.S., Marginean, R., Nomura, K.,Rudigier, M., Mihai, R., Werner, V., Carroll, R. J., Gurgi, L. A., Oprea, A., Berry, T., Serban, A., C. R. Nita, C. R., Sotty, C., Suvaila, R., Turturica, A., Costache, C., Stan, L., Olacel, A., Boromiza, M. and Toma, S. (2017). Gamma-ray spectroscopy of low-lying excited states and shape competition in $^{194}$Os, *Physical Review* .C 95, 024328, 1-9.

Ertugral, F., Guliyev, E., Kuliev, A.A. (2015) Quadrupole Moments and Deformation Parameters of the $^{166\text{-}180}$Hf, $^{180\text{-}186}$W and $^{152\text{-}168}$Sm Isotopes, *A. Phys. Pol*., B128, 254-257

Flavigny, F., Chung, X. L., Linh, B. D. (2017) Shape Evolution in Neutron-rich Krypton Isotopes beyond N = 60 : First spectroscopy of 98,100Kr, *Physical Review Letters*. DOI: 10.1103/PhysRevLett.118.242501

Garcia-Ramos J.E., and Heyde, K., (2013). Nuclear shape coexistence: A study of the even-even Hg isotopes using the interacting boson model with configuration mixing *Phys. Rev*. C89, 014306. DOI:10.1103/PhysRevC.89.014306.

Garcia-Ramos, J.E., Heyde, K., Robledo, L.M., and Rodrıguez-Guzman. R. (2014). Shape evolution and shape coexistence in Pt isotopes: comparing interacting boson model configuration mixing and Gogny mean-field energy surfaces.*Phys.Rev.* C89 no.3, 034313 DOI: 10.1103/PhysRevC.89.034313

Henley, E. M., and Garcia, A. (2007). Subatomic physics, 3rd Edition. World Scientific Publishing Co. *Pte. Ltd.*

Hodgson, P. E. and Gagioli, E. (1997). Introductory Nuclear Physics, ISBN 0-19-851897-8, Oxford Science Publications, New York

Krane, K. S. (1988). Introductory Nuclear Physics, revised edition, John Wiley and Sons, Inc., New York.

NuDat2.6, Retrieved (2018). National Nuclear Data Center, Brookhaven National Laboratory. www.nndc.bnl.gov/Nudat2.6

Otsuka, T. and Tsunoda, Y. (2016). The role of shell evolution in shape coexistence. *J. Phys. G: Nucl. Part. Phys.* 43, 024009, 1-18W. DOI:10.1088/0954-3899/43/2/024009

Pritychenko, B., Birch, M., Singh, B. and Horoi, M. (2016). Tables of E2 transition probabilities from the first $2^+$states in even–even nuclei, *ELSEVIER* 107: 1–139

Raman, S. (2002). A Tale of Two Compilations: Quadrupole Deformations and Internal Conversion Coefficients, *Journal of Nuclear Science and Technology*, 39: sup2, 450-454. DOI: 10.1080/00223131.2002.10875137.

Regan P. H. (2003). Post Graduate Nuclear Experimental Techniques (4NET), University of Surrey, Guildford, UK. Unpublished.

Segre chart, (2019). The chemogenesis web-book. https://www.metasynthesis.com/webbook/33_segre/segre.html

Wong, S.M. (2004). Introductory Nuclear Physics, Second Edition, Wiley-VchVerlagGmbII& Co. KGaA, Weinheim.